Atomic Structure and Bonding of Boron-Induced Reconstructions on Si(001)

Yajun Wang and Robert J. Hamers*

Department of Chemistry, University of Wisconsin-Madison, 1101 University Avenue, Madison, Wisconsin 53706

Efthimios Kaxiras

Department of Physics and Division of Applied Science, Harvard University, Cambridge, Massachusetts 02138

Scanning tunneling microscopy (STM) and tunneling spectroscopy have been used to investigate the local structural and electronic properties of boron-induced reconstructions on Si(001). Thermal decomposition of diborane produces three ordered reconstructions, which arise from ordered arrangements of three structural subunits, with a local boron coverage of $\frac{1}{2}$ monolayer. A structural model is proposed which accounts for the observed STM features. The principal structural subunit is shown to be an ordered arrangement of four boron atoms at substitutional sites in the first bulklike silicon layer, which is then capped with ordered arrangements of silicon dimers and dimer vacancies.

Doping of semiconductor structures is a strongly nonequilibrium process involving a complex interplay of surface structure and chemical kinetics. Recent investigations have shown that the interfacial chemistry of boron with silicon permits the fabrication of narrow, nonequilibrium two-dimensional layers of highly doped silicon with high structural and electrical quality [1–8]. The growth of such nonequilibrium structures by chemical techniques presents a novel method for preparation of nanometer-scale electronic devices based on self-limiting interfacial chemistry. In this Letter, we report the first scanning tunneling microscopy (STM) studies of boron-induced reconstructions and the formation of δ-doped layers on Si(001). Our results show that boron interacts with Si(001) to produce several complex, ordered reconstructions which can be described as arrangements of three basic structural subunits. A detailed analysis of the STM results, in conjunction with other electrical and chemical probes of the surface, provides new insight into the structure and bonding within boron δ-doped layers.

Si(001) samples (Wacker) were cleaned by annealing at 1425 K in ultrahigh vacuum. These were imaged with the STM to ensure a well-ordered starting surface and were then typically exposed to 1% diborane in He [5000 L, where 1 langmuir (L) = 10^{-6} torr sec] or pure decaborane (0.1-1 L) at 815 K followed by annealing at 1000 K for 90 sec. Both diborane and decaborane produced similar structures.

While the clean Si(001) surface has large, flat terraces, Fig. 1 shows that exposure to diborane at elevated temperatures produces islands atop the terraces. These islands as well as many smaller regions of the substrate (thirteen regions in Fig. 1, labeled "RS") exhibit a complex boron-induced surface reconstruction. The boron-reconstructed regions are separated by regions of clean Si(001)-(2 × 1), leading to a striking spatial segregation of boron into regions of high concentration (evidenced by local reconstructions) and regions of nearly clean (undoped) Si.

Figure 2 shows high-resolution STM images of the boron-induced reconstructions. In Fig. 2(a), small regions showing $c(4 \times 4)$ symmetry (square unit cell rotated 45°, labeled "α") and (4×4) symmetry (square unit cell, labeled "γ") can be observed. Additionally, some regions showing the (2×1) reconstruction of the "clean" Si(001) surface can be observed (rectangular unit cell, labeled "Si"). The local electronic structure of these reconstructions is revealed by comparing images probing the occupied and unoccupied electronic states of a single area, as shown in Figs. 2(b) (occupied states, −2 V sample bias) and 2(c) (unoccupied states, +2 V bias). In Figs. 2(b) and 2(c), the surface again shows primarily the $c(4 \times 4)$
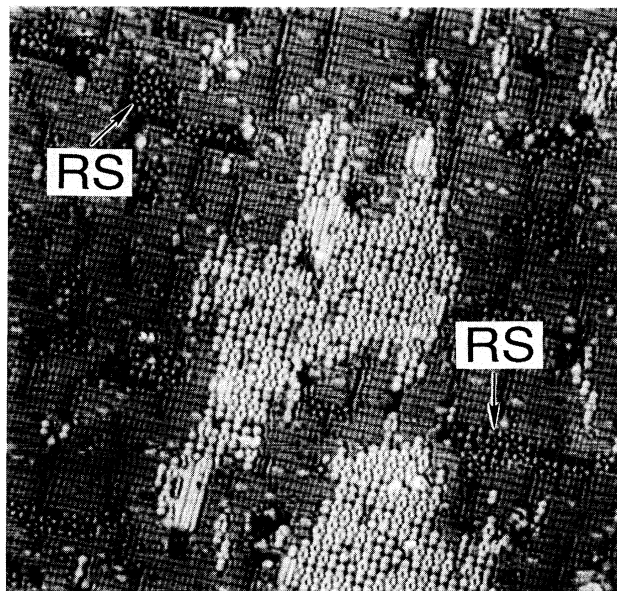

FIG. 1. STM image of diborane-exposed surface showing formation of reconstructed islands and patchy reconstruction of substrate terrace. $V_{\text{sample}} = +2.0$ V; $I_{\text{tunnel}} = 0.2$ nA.
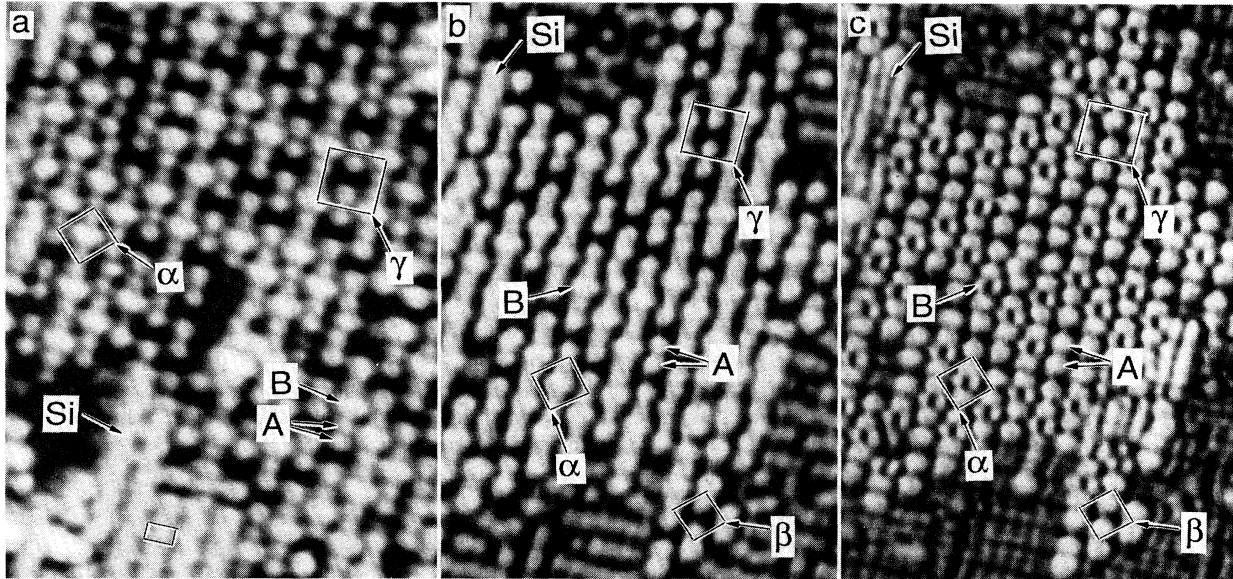
FIG. 2.   High-resolution images of boron-induced reconstructions on Si(001) surface. α, β, and γ denote α-c (4 × 4), β-c (4 × 4), and γ-(4 × 4) unit cells of observed reconstructions; A and B denote structural subunits of reconstructions, as described in text. (a) High-resolution image showing boron-induced reconstruction and region of clean Si(001)-(2 × 1), with (2 × 1) unit cell outlined. (b) High-resolution imaging of occupied surface electronic states. Image area 104 Å × 157 Å; $V_{sample} = -2.0$ V; $I_{tunnel} = 0.2$ nA. (c) Image showing identical region as (b) but tunneling into unoccupied electronic states. Image area 104 Å × 157 Å; $V_{sample} = +2.0$ V; $I_{tunnel} = 0.2$ nA.

reconstruction, with a few unit cells of (4 × 4) symmetry. Additionally, small regions exhibiting yet another reconstruction of c (4 × 4) symmetry can be observed, labeled "β." For clarity, we will refer to the most common structure of c (4 × 4) symmetry as "α-c (4 × 4)," the less common c (4 × 4) reconstruction as "β-c (4 × 4)," and the (4 × 4) reconstruction as "γ-(4 × 4)."

Close inspection shows that all three boron-induced reconstructions share common structural features. We consider first the most common, the α-c(4 × 4) reconstruction. At negative sample bias each unit cell contains two equivalent oval-shaped protrusions and a single, unique oval protrusion which under these conditions appears 0.35 Å higher. Although the highest-symmetry unit cell can be described as a single high oval protrusion bounded on each side by a single lower oval, examination of the top and bottom edges of the island in Figs. 2(b) and 2(c) shows that the edges of reconstructed areas always terminate with a *pair* of the lower protrusions. Thus, the α-c(4 × 4) reconstruction is best described in terms of two structural building blocks: a pair of two equivalent oval-shaped protrusions, labeled "A" in Fig. 2, and a single unique oval-shaped protrusion, labeled "B" in Fig. 2. This structure consisting of one A subunit and one B subunit repeats every $4a_0$ (where $a_0 = 3.84$ Å) along the $\langle 1\bar{1}0 \rangle$ direction and is ordered between adjacent rows in c (4 × 4) symmetry as indicated in Fig. 2. At positive bias, Fig. 2(c) shows that the B feature splits into two well-resolved nearly circular protrusions, and the two oval-shaped protrusions constituting the A feature now appear 0.4 Å higher than the B feature, but otherwise unchanged in

appearance. The changes in appearance of the B features as a function of bias are very similar to those exhibited by dimers of the clean Si(001) surface, suggesting a common origin.

The γ-(4 × 4) reconstruction is nearly identical to the α-c (4 × 4), except that half the B features appear to be replaced by vacancies.

Finally, the β-c (4 × 4) reconstruction visible at lower right in Figs. 2(b) and 2(c) arises from an ordered arrangement of the A features alone. Within each β-c (4 × 4) unit cell, the two ovals are separated along the $\langle 1\bar{1}0 \rangle$ direction by a distance alternating between 5.0 and 10.4 Å (compared with $a_0 = 3.84$ Å), such that the ovals slow a clear grouping into pairs. The shape, grouping, and apparent height of the oval protrusions in the β-c (4 × 4) reconstruction are nearly identical to those of the "lower" oval protrusions in the α-c (4 × 4) and β-c (4 × 4) reconstructions, indicating that the A subunit is common to all three.

Further insight is provided by STM measurements which show that exposing Si(001) to much smaller amounts of B_2H_6 (50 L) produces *only* the A features, while at intermediate exposures (100–500 L) these group together (alone and with the B features) to form the various ordered reconstructions. These results confirm that the A feature is the primary boron-induced surface feature and that this *same* feature is contained in all three boron-induced reconstructions. Additionally, the features reported here are not produced at sample temperatures below 755 K, indicating substantial atomic rearrangement.

To determine the local boron coverage within the re-constructed regions, Auger electron spectra were obtained on a number of samples exposed to diborane. The B/Si peak ratio of the B/Si(001) samples was compared with that for the Si(111)-($\sqrt{3} \times \sqrt{3}$)B reconstruction, which arises at $\frac{1}{3}$ monolayer B [9,10], and corrections were applied based on the fractional area occupied by the reconstructions measured *in situ* with STM. These mea-surements showed that the B coverage within the recon-structed B/Si(001) regions was 0.56 ± 0.05 monolayer, or a coverage of $\frac{1}{2}$, in agreement with previous studies of δ-doped B/Si(001) [3–8,11,12].

The electronic properties of these layers were charac-terized in two ways. Figure 3 shows the results of local tunneling spectra at two locations within the α-c (4 × 4) regions. Spectra measured over the bright B subunits show a band gap of approximately 0.7 eV with the Fermi level (E_F) in the lower part of the surface-state gap, similar to spectra obtained on dimers of clean Si(001). In contrast, spectra measured directly above the A features show a high current (a high state density) just below E_F, with a 0.5 eV gap above. This high state density just below E_F is what one would expect if the A features act as electron acceptors (p-type dopants) pinning the Fermi level near the valence band edge. Local surface photovoltage (SPV) measurements of these layers on n-type substrates further showed that when measured over the clean Si regions the local SPV, normally positive on n-type samples, becomes more negative and shows local p-type doping as the recon-structed area increases.

Figure 4 shows a structural model we have devel-oped for the boron-induced reconstructions. The STM studies show that only the A feature is observed at low coverage, and this feature alone is common to all three boron-induced reconstructions. The 0.5 monolayer boron coverage requires that each A feature results from four boron atoms, while p-type doping behavior and the high temperature required to form the reconstructions suggest a substitutional location. The STM images directly reveal
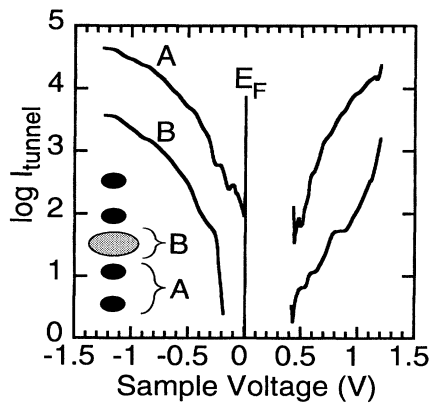
the symmetry of the A features with respect to the Si(001) lattice, strongly constraining the possible boron positions. Finally, previous studies [2,3,7,8] have shown that epi-taxial silicon can be grown atop these δ-doped layers at low temperatures, so that any proposed model must al-low for this possibility. We propose that the A features arise from Si dimers bonded above a Si(001) surface in which half the Si atoms in the first bulklike layer are re-placed by boron at the positions indicated in Fig. 4, and that the two oval-shaped features within each A subunit arise from electronic states associated with these "boron-bonded" dimers and their Si—B bonds.

The B features show changes in appearance with applied bias that are identical to those for Si=Si dimers of the clean surface, and the tunneling I-V spectra are also very similar. Likewise, the bonding location of feature B is consistent with its interpretation as a Si=Si dimer. We propose that the B feature arises from a Si=Si dimer bonded to four second-layer Si atoms in a local environment similar to that of the clean Si(001) surface.

With this model, all three reconstructions can be de-scribed as ordered combinations of the A and B structural subunits together with dimer vacancies, and all three have $\frac{1}{2}$ monolayer boron coverage. The common α-c (4 × 4) reconstruction arises from one A subunit and one B subunit in each unit cell, as depicted in Fig. 4. The β-c (4 × 4) reconstruction arises from one A subunit and one dimer vacancy in each unit cell, while the γ-(4 × 4) reconstruction is obtained by replacing only half of the B subunits (Si=Si dimers) with dimer vacancies, leading to a larger unit cell containing two A subunits, one B subunit, and one dimer vacancy. We expect that second-layer Si atoms exposed at dimer vacancies in the
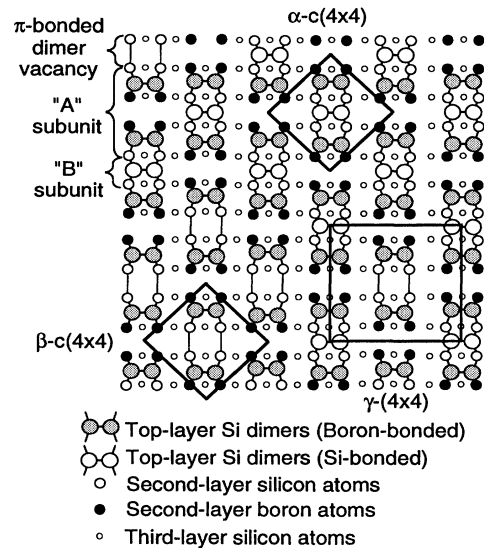
FIG. 3. Local tunneling spectroscopy measurements acquired above the A and B structural subunits. Curves have been displaced vertically for clarity.

FIG. 4. Structural subunits of boron-induced reconstruc-tions and proposed arrangements of these subunits to form α-c (4 × 4), β-c (4 × 4), and γ-(4 × 4) unit cells.

γ-(4×4) reconstruction are rebonded [13,14] and have included these interactions in Fig. 4.

The differences in appearance between the boron-bonded Si dimers of the A subunit and the silicon-bonded dimers of the B subunits are attributed to a combination of structural and electronic effects. Calculations for SiH_3BH_2, $(SiH_3)_2BH$, and $(SiH_3)_3B$ [15] and experimental measurements for the Si(111)-$(\sqrt{3} \times \sqrt{3})$B reconstruction [9,10] and for δ-doped B/Si(001) layers [8] indicate Si—B bond lengths of 2.0–2.1 Å, substantially shorter than the 2.35 Å bond length in bulk silicon. Thus, boron substitution at the Si(001) surface will distort the Si lattice to achieve a short B—Si bond. In our model, a shortened B—Si bond can be achieved by breaking the weak π bond of the boron-bonded Si dimers; this might explain why the A features fail to show the splitting at positive bias that is characteristic of π-bonded dimers. Breaking the π bond would also facilitate electron transfer from silicon to boron, in agreement with tunneling spectroscopy and SPV measurements. Filled-state STM images then likely reflect the position of the B—Si backbonds and possibly the fourth sp^3-hybridized boron dangling bond which, normally empty, could be partially filled due to charge transfer from Si. These dangling bonds on adjacent boron atoms might further interact to form B—B σ-bonds (not depicted in Fig. 4). The above interpretation also explains why in filled-state images the A features appear lower than the B features, even though the A features show a high state density just below E_F: The STM images contain both geometric and electronic information, and, although the A features have a high state density just below E_F, the B—Si and partially filled B "dangling bonds" are geometrically lower than the B-type Si=Si dimers.

The self-consistency of our model can be checked by measuring the areas of the reconstructed islands and terraces. Each α-c (4×4) unit cell will eject six Si atoms if formed in the substrate plane, but requires addition of two Si atoms to form as an island. If this is the primary B-induced reconstruction, then, according to our model at high boron exposure, the islands should occupy 75% of the surface area. Although a quantitative measurement is complicated by multiple reconstructions, our measurements do show that at high exposure the reconstructed islands occupy approximately 75% of the total surface area. At low exposure, STM images show only the A units, which constitute the β-c (4×4) reconstruction. In our model forming an A unit as an "island" structure does not require any net gain or loss of Si. The extra Si required to form α-c (4×4) and γ-(4×4) islands most likely originates by detachment from steps or by ejection from the terraces during boron incorporation; then, conditions that favor low Si adatom concentration (low temperature, low exposure) should favor the formation of the β-c (4×4) reconstruction, in agreement with our results.

Our results are generally consistent with previous studies of δ-doped B/Si(001) layer formation using other

precursors [1–8]. Although these previous studies have shown (2×1) diffraction patterns in low energy electron diffraction (LEED) [1,3–5], the arrangement of Si=Si dimers and vacancies we observe in the STM typically leads to domain sizes of only 20–30 Å. Since LEED samples order over >100 Å, only the shorter-range (2×1) periodicity is observable in this technique.

Our investigations have shown that the interaction of boron with Si(001) is strongly heterogeneous. Based on the experimental data we have developed an atomistic model of the structure and bonding of boron on the Si(001) surface and the formation of two-dimensional "delta-doped" layers. Our work provides new insight into structure, bonding, and electronic properties of the boron-silicon system.

---

*Author to whom all correspondence should be addressed. Electronic address: Hamers@BERT.CHEM.WISC.EDU

[1] M. L. Yu, D. J. Vitkavage, and B. S. Meyerson, J. Appl. Phys. **59**, 4032 (1986).

[2] B. S. Meyerson, F. K, LeGoues, T. N. Nguyen, and D. L. Harame, Appl. Phys. Lett. **50**, 113 (1987).

[3] R. L. Headrick, B. E. Weir, A. F. J. Levi, D. J. Eaglesham, and L. C. Feldman, Appl. Phys. Lett. **57**, 2779 (1990).

[4] R. L. Headrick, B. E. Weir, A. F. J. Levi, B. Freer, J. Bevk, and L. C. Feldman, J. Vac. Sci. Technol. A **9**, 2269 (1991).

[5] R. L. Headrick, B. E. Weir, A. F. J. Levi, D. J. Eaglesham, and L. C. Feldman, J. Cryst. Growth **111**, 838 (1991).

[6] D. D. Koleske, S. M. Gates, and D. B. Beach, J. Appl. Phys. **72**, 4073 (1992).

[7] B. E. Weir, B. S. Freer, R. L. Headrick, D. J. Eaglesham, G. H. Gilmer, J. Bevk, and L. C. Feldman, Appl. Phys. Lett. **59**, 204 (1991).

[8] B. E. Weir, R. L. Headrick, Q. Shen, L. C. Feldman, M. S. Hybertsen, M. Needels, M. Schluter, and T. R. Hart, Phys. Rev. B **46**, 12 861 (1992).

[9] R. L. Headrick, I. K. Robinson, E. Vlieg, and L. C. Feldman, Phys. Rev. Lett. **63**, 1253 (1989).

[10] E. Kaxiras, K. C. Pandey, F. J. Himpsel, and R. M. Tromp, Phys. Rev. B **41**, 1262 (1990).

[11] S. M. Gates and D. D. Koleske, Appl. Phys. Lett. **61**, 309 (1992).

[12] C. P. Parry, R. A. Kubiak, S. M. Newstead, T. E. Whall, and E. H. C. Parker, J. Appl. Phys. **71**, 118 (1992).

[13] K. C. Pandey, in *Proceedings of the Seventeenth International Conference on the Physics of Semiconductors*, edited by J. D. Chadi and W. J. Harrison (Springer-Verlag, New York, 1985).

[14] R. J. Hamers, R. M. Tromp, and J. E. Demuth, Phys. Rev. B **34**, 5343 (1986).

[15] C. W. Bock, M. Trachtman, and G. J. Mains, J. Phys. Chem. **89**, 2283 (1985).
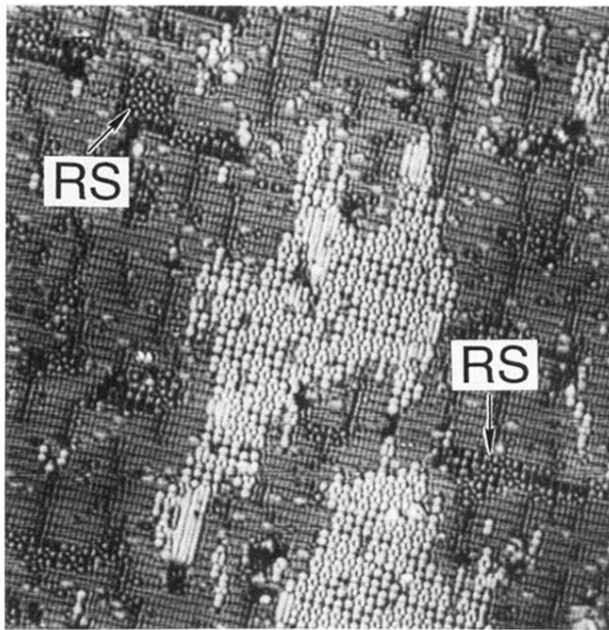
FIG. 1. STM image of diborane-exposed surface showing formation of reconstructed islands and patchy reconstruction of substrate terrace. $V_{sample} = +2.0$ V; $I_{tunnel} = 0.2$ nA.
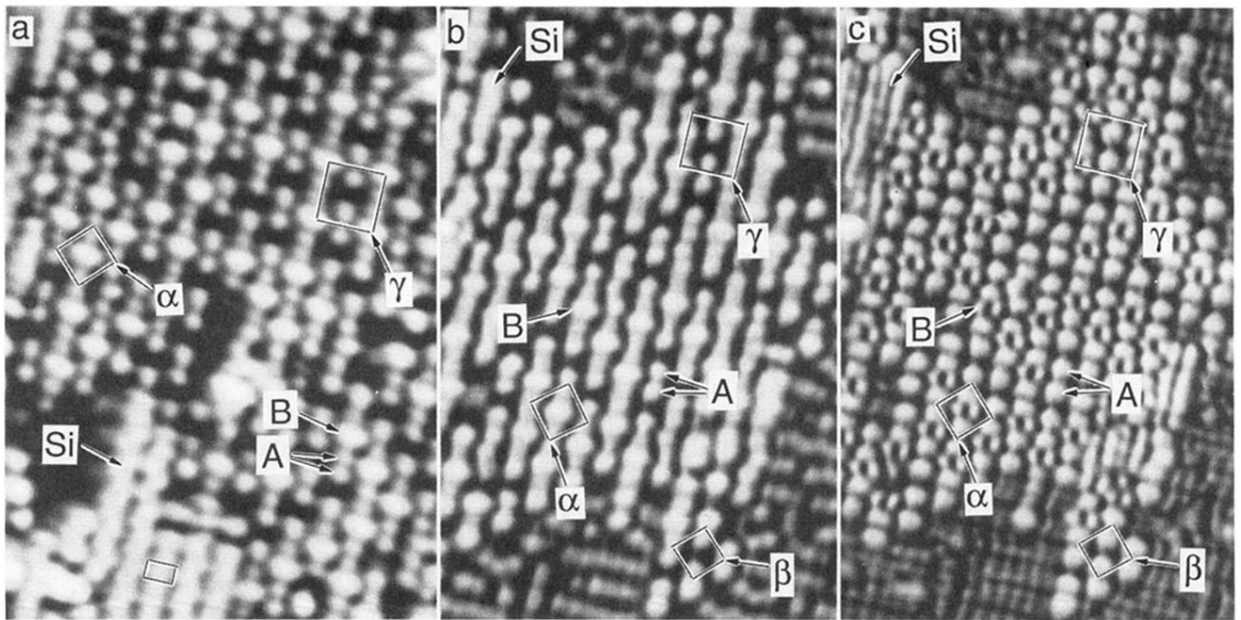
FIG. 2. High-resolution images of boron-induced reconstructions on Si(001) surface. α, β, and γ denote α-c (4 × 4), β-c (4 × 4), and γ-(4 × 4) unit cells of observed reconstructions; A and B denote structural subunits of reconstructions, as described in text. (a) High-resolution image showing boron-induced reconstruction and region of clean Si(001)-(2 × 1), with (2 × 1) unit cell outlined. (b) High-resolution imaging of occupied surface electronic states. Image area 104 Å × 157 Å; $V_{sample} = -2.0$ V; $I_{tunnel} = 0.2$ nA. (c) Image showing identical region as (b) but tunneling into unoccupied electronic states. Image area 104 Å × 157 Å; $V_{sample} = +2.0$ V; $I_{tunnel} = 0.2$ nA.